Condensed Matter Physics, 2013, Vol. 16, No 3, 33701: 1–10
DOI: 10.5488/CMP.16.33701
http://www.icmp.lviv.ua/journal

Optimization of quantum cascade laser operation by geometric design of cascade active band in open and closed models

M.V. Tkach*, Ju.O. Seti, I.V. Boyko, O.M. Voitsekhivska
Chernivtsi National University, 2 Kotsyubinsky St., 58012 Chernivtsi, Ukraine

Received November 20, 2012

Using the effective mass and rectangular potential approximations, the theory of electron dynamic conductivity is developed for the plane multilayer resonance tunnel structure placed into a constant electric field within the model of open nanosystem, and oscillator forces of quantum transitions within the model of closed nanosystem. For the experimentally produced quantum cascade laser with four-barrier active band of separate cascade, it is proven that just the theory of dynamic conductivity in the model of open cascade most adequately describes the radiation of high frequency electromagnetic field while the electrons transport through the resonance tunnel structure driven by a constant electric field.

Key words: *resonance tunnel nanostructure, conductivity, quantum cascade laser*

PACS: *73.40.Gk, 85.30.Mn, 81.07.St*

1. Introduction

It is well known that the operation of quantum cascade laser (QCL) [1–4], quantum cascade detector (QCD) [5–7] and other appropriately operating nanodevices is based on the transport properties of open multilayer nanostructures. In spite of the long period of investigations into electron transport through the resonance tunnel structures (RTS), taking into account the interaction of electronic current with constant electric and high frequency electromagnetic fields, the current theory is still far from being well correlated with experimental data.

The main problems in elaborating a consistent theory of electron transport through the RTS are the mathematical difficulties arising when solving the non-stationary Schrodinger equation with Hamiltonians for even comparatively simple models with open boundaries which allow the infinite movement of quasi-particles. In order to avoid these difficulties, the evaluations obtained for the closed analogues of open RTS with rectangular potential wells and barriers were used in early papers [2–4] for the theory of electron transport through the QCL active bands. The closed models did not make it possible to study the currents due to the stationary electron states but they satisfactorily described the electron spectrum and, thus, the energies of electromagnetic radiation and wave functions which were used for the calculation of dipole moments of quantum transitions.

Active bands of QCL, such as open two- and three-barrier RTS, were theoretically studied in [8–10]. In these papers, the non-stationary one-dimensional Schrodinger equation describing the electron transport through the RTS with δ-like potential barriers was solved taking into account the interaction with constant electric and high frequency electromagnetic fields. The simplified model of a constant effective mass of an electron along the whole nanosystem and δ-barrier approximation of the potential made it possible to calculate and investigate the electronic currents and, consequently, to calculate the dynamic conductivity in ballistic regime when the biggest lifetimes in operating quasi-stationary states were much

* E-mail: ktf@chnu.edu.ua

smaller than the relaxation times for the electron energy due to the dissipative processes (phonons, impurities and so on).

The δ-barrier model for an open RTS [11, 12] essentially overestimates the resonance widths of operating quasi-stationary states compared to the more adequate model of rectangular potentials. It explained some properties of electron transport but could not be used as a reliable base to be compared with the experimental data and, thus, to optimize the geometric design of QCL active band.

According to the abovementioned and using the effective mass and rectangular potential approximations, in this paper we develop the theory of quasi-stationary spectrum and dynamic conductivity of the electrons interacting with high frequency electromagnetic field within the model of open multilayer RTS and stationary spectrum together with oscillator forces of quantum transitions within the model of closed RTS in a constant electric field. We use the obtained theoretical results in order to calculate the energy of electromagnetic radiation for the experimentally produced QCL [3] with a four-barrier active band of a separate cascade. The comparison of numerical and experimental data illustrates the capabilities of different models in optimizing the active band geometric design.

2. Theory of dynamic conductivity of a resonance tunnel cascade with four-barrier active band and oscillator forces of quantum transitions in closed model

The separate cascade of QCL such as RTS, containing a four-barrier active band and injector consisting of a certain number of plane nanolayers (wells and barriers) having fixed sizes, figure 1, is studied within two models: open (o) and closed (c). The constant electric field with intensity F is applied perpendicularly to the RTS planes. For the open model, we assume that the monoenergetic current of non-interacting electrons having energy E and concentration n0 impinges at RTS from the left hand side, perpendicularly to its planes. Under these conditions and taking into account the small difference between the lattice constants of wells and barriers, the problem settles to the study of one-dimensional electron transport using the models of effective mass and rectangular potentials.

Taking the coordinate system as it is shown in figure 1, the effective mass and potential energy of an

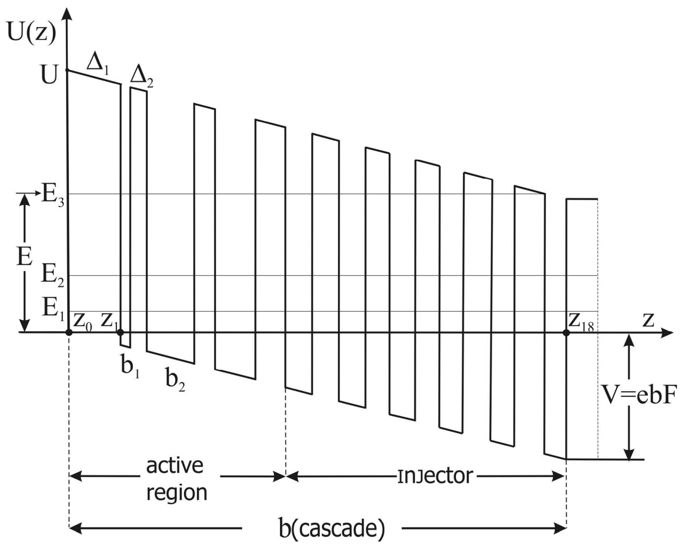

Figure 1. The energy scheme of separate cascade with four-barrier active region and injector. The widths of the barriers (Δ_p): 5.0, 1.5, 2.2, 3.0, 2.3, 2.2, 2.0, 2.3, 2.8 and widths of the wells (b_p): 0.9, 4.7, 4.0, 2.3, 2.2, 2.0, 2.0, 1.9, 1.9 are presented from the left to the right in nm units.

electron in open (o) or closed (c) RTS (without the field) is conveniently written as

$$m_{\left\{ {\rm o} \atop {\rm c} \right\}}(z) = \left\{ \begin{array}{c} m_0 \\ m_1 \end{array} \right\} [\theta(-z)+\theta(z-b)] + m_0 \sum_{p=1}^{N_{\rm W}} \left[\theta(z-z_{2p-1})-\theta(z-z_{2p})\right] + m_1 \sum_{p=0}^{N_{\rm B}-1} \left[\theta(z-z_{2p})-\theta(z-z_{2p+1})\right], \tag{1}$$

$$U_{\left\{ {\rm o} \atop {\rm c} \right\}}(z) = \left\{ \begin{array}{c} 0 \\ U \end{array} \right\} [\theta(-z)+\theta(z-b)] + U \sum_{p=0}^{N_{\rm B}-1} \left[\theta(z-z_{2p})-\theta(z-z_{2p+1})\right], \tag{2}$$

where $N_{\rm W}$, $N_{\rm B}$ are the numbers of wells and barriers in the RTS which correspond to the active band or to the whole cascade, depending on the model.

In order to observe the electron transport through the RTS, the latter should be obligatory an open one. Thus, a dynamic conductivity arises when quasi-stationary states are present in a nanosystem. Developing the theory of RTS active conductivity within the open model, we study the properties of electron stationary spectrum and oscillator forces of quantum transitions within the closed model in order to be compared. The widths of outer barriers of active band (or cascade) in the closed model limit to the physical infinity and the constant electric field is applied inside the nanosystem only. The reason to study the closed model is that the similar model is, evidently, the theoretical base of the choice of experimental geometric design of QCL cascade with active band and injector [3]. We are going to compare the experimental data with our results obtained within the model of open RTS.

In order to calculate the dynamic conductivity within the open model and oscillator forces within the closed one, we first solve the stationary Schrodinger equations

$$H_{\left\{ {\rm o} \atop {\rm c} \right\}}(z)\Psi_{\left\{ {\rm o} \atop {\rm c} \right\}}(z) = E\Psi_{\left\{ {\rm o} \atop {\rm c} \right\}}(z) \tag{3}$$

with the Hamiltonian of an electron in RTS driven by a constant electric field

$$H_{\left\{ {\rm o} \atop {\rm c} \right\}} = -\frac{\hbar^2}{2}\frac{\partial}{\partial z} m^{-1}_{\left\{ {\rm o} \atop {\rm c} \right\}}(z)\frac{\partial}{\partial z} - eF\left(z[\theta(z)-\theta(z-b)] - \left\{ \begin{array}{c} b \\ 0 \end{array} \right\}\theta(z-b)\right). \tag{4}$$

The solutions of equations (3) are written as follows:

$$\Psi_{\left\{ {\rm o} \atop {\rm c} \right\}}(z) = \Psi^{(0)}_{\left\{ {\rm o} \atop {\rm c} \right\}}(z)\theta(-z) + \sum_{p=1}^{N_{\rm W}+N_{\rm B}} \Psi^{(p)}_{\left\{ {\rm o} \atop {\rm c} \right\}}(z)\left[\theta(z-z_{p-1})-\theta(z-z_p)\right] + \Psi^{(N_{\rm W}+N_{\rm B}+1)}_{\left\{ {\rm o} \atop {\rm c} \right\}}(z)\theta(z-b), \tag{5}$$

where the wave functions

$$\Psi^{(0)}_{\left\{ {\rm o} \atop {\rm c} \right\}}(z) = A^{(0)}_{\left\{ {\rm o} \atop {\rm c} \right\}} {\rm e}^{\left\{ {\rm i}k \atop \chi \right\} z} + B^{(0)}_{\left\{ {\rm o} \atop {\rm c} \right\}} {\rm e}^{-\left\{ {\rm i}k \atop \chi \right\} z}, \tag{6}$$

$$\Psi^{(p)}_{\left\{ {\rm o} \atop {\rm c} \right\}}(z) = A^{(p)}_{\left\{ {\rm o} \atop {\rm c} \right\}} {\rm Ai}(\xi_p(z)) + B^{(p)}_{\left\{ {\rm o} \atop {\rm c} \right\}} {\rm Bi}(\xi_p(z)), \qquad [p = 1 \div (N_{\rm W}+N_{\rm B})], \tag{7}$$

$$\Psi^{(N_{\rm W}+N_{\rm B}+1)}_{\left\{ {\rm o} \atop {\rm c} \right\}}(z) = A^{(N_{\rm W}+N_{\rm B}+1)}_{\left\{ {\rm o} \atop {\rm c} \right\}} {\rm e}^{\left\{ {\rm i}K \atop \chi \right\} z} + B^{(N_{\rm W}+N_{\rm B}+1)}_{\left\{ {\rm o} \atop {\rm c} \right\}} {\rm e}^{-\left\{ {\rm i}k \atop \chi \right\} z} \tag{8}$$

are the superpositions of the exact linearly independent solutions of equations (3) in the respective ranges of z variable. Here, we introduced the notations

$$k = \hbar^{-1}\sqrt{2m_0 E}, \qquad \chi = \hbar^{-1}\sqrt{2m_1(U-E)}, \qquad K = \hbar^{-1}\sqrt{2m_0(E+V)}, \qquad V = eFb,$$

$$\xi_p(z) = \left\{ \begin{array}{ll} +\left(\frac{2m_1 V b^2}{\hbar^2}\right)^{\frac{1}{3}} \left(\frac{U-E}{V} - \frac{z}{b}\right), & p = 1, 3, 5, \dots, \\ -\left(\frac{2m_0 V b^2}{\hbar^2}\right)^{\frac{1}{3}} \left(\frac{E}{V} - \frac{z}{b}\right), & p = 2, 4, 6, \dots . \end{array} \right. \tag{9}$$

$\mathrm{Ai}(\xi)$, $\mathrm{Bi}(\xi)$ are the Airy functions.

The conditions of a wave function and its density of current continuity should be fulfilled at all nanosystem interfaces in the both models

$$\Psi^{(p)}_{\{\substack{\mathrm{o}\\ \mathrm{c}}\}}(z_p)=\Psi^{(p+1)}_{\{\substack{\mathrm{o}\\ \mathrm{c}}\}}(z_p), \qquad \left.\frac{\mathrm{d}\Psi^{(p)}_{\{\substack{\mathrm{o}\\ \mathrm{c}}\}}(z)}{m_{\{\substack{\mathrm{o}\\ \mathrm{c}}\}}(z)\mathrm{d}z}\right|_{z=z_p-\varepsilon}=\left.\frac{\mathrm{d}\Psi^{(p+1)}_{\{\substack{\mathrm{o}\\ \mathrm{c}}\}}(z)}{m_{\{\substack{\mathrm{o}\\ \mathrm{c}}\}}(z)\mathrm{d}z}\right|_{z=z_p+\varepsilon}, \tag{10}$$

$p=0\div(N_{\mathrm{W}}+N_{\mathrm{B}})$, $\varepsilon\to+0$.

The wave functions tend to zero at $z\to\pm\infty$ in the closed model, since $B^{(0)}_{(\mathrm{c})}=A^{(N_{\mathrm{W}}+N_{\mathrm{B}}+1)}_{(\mathrm{c})}=0$. Thus, the system of equations (10) brings us to the dispersion equation, consistently determining the energy spectrum (E_n) and all coefficients $A^{(p)}_{(\mathrm{c})}$, $B^{(p)}_{(\mathrm{c})}$ through one of them. The latter is obtained from the normality condition

$$\int\limits_{-\infty}^{\infty}\Psi^{*}_{(\mathrm{c})n}(z)\Psi_{(\mathrm{c})n'}(z)\mathrm{d}z=\delta_{nn'}\,. \tag{11}$$

Now, the electron wave functions $\Psi_{(\mathrm{c})n}(z)$ and energies (E_n) of all stationary states are defined in the closed model. Using them, the oscillator forces of quantum transitions between the states n and n' can be calculated within the formula

$$f_{nn'}=\frac{2(E_n-E_{n'})\overline{m}_{(\mathrm{c})}}{\hbar^2}\left|\int\limits_{-\infty}^{\infty}\Psi^{*}_{(\mathrm{c})n}(z)\,z\,\Psi_{(\mathrm{c})n'}(z)\mathrm{d}z\right|^2. \tag{12}$$

For the open model, there should be no backward wave from the right of a nanosystem, since $B^{(N_{\mathrm{W}}+N_{\mathrm{B}}+1)}_{(\mathrm{o})}=0$. All coefficients $A^{(p)}_{(\mathrm{o})}$, $B^{(p)}_{(\mathrm{o})}$ of the wave function $\Psi_{(\mathrm{o})}(z)$ are found from the condition (10) through one of them, in its turn, defined by the incident density of the current impinging at RTS from the left hand side. In this case, the electron spectrum is the quasi-stationary one with the resonance energies (E_n) and resonance widths ($\Gamma_n=\hbar\tau_n^{-1}$) where τ_n is the lifetime in the n-th quasi-stationary state. The resonance energies are fixed by the maxima of a probability distribution function of an electron inside RTS (in energy scale E)

$$W(E)=\frac{1}{b}\int\limits_{0}^{b}\left|\Psi_{(\mathrm{o})}(E,z)\right|^2\mathrm{d}z. \tag{13}$$

The resonance widths (Γ_n) are fixed by the widths of this function at the halves of its maxima placed at the respective resonance energies E_n.

The quantum transitions between the quasi-stationary states occur when the electrons transport through the open RTS placed into the electric field. Consequently, the electromagnetic field with the respective frequency arises. Its intensity is proportional to the magnitude of the dynamic conductivity. In the quantum transitions accompanied by the absorption of electromagnetic energy, the positive dynamic conductivity is formed and, during the radiation of electromagnetic energy, the negative dynamic conductivity of RTS is formed.

In order to calculate the negative conductivity of open RTS operating in a laser regime, one has to obtain the wave functions of electrons interacting with the electromagnetic field. It is found from the time-dependent Schrödinger equation:

$$\mathrm{i}\hbar\frac{\partial\Psi(z,t)}{\partial t}=\left[H_{(\mathrm{o})}(z)+H(z,t)\right]\,\Psi(z,t), \tag{14}$$

where $H_{(\mathrm{o})}(z)$ is the Hamiltonian (4) for the electrons in RTS without the electromagnetic field and

$$H(z,t)=-e\mathscr{E}\{z\,[\theta(z)-\theta(z-b)]+b\theta(z-b)\}\left(\mathrm{e}^{\mathrm{i}\omega t}+\mathrm{e}^{-\mathrm{i}\omega t}\right) \tag{15}$$

is the Hamiltonian of electrons interacting with time-dependent electromagnetic field characterized by the frequency ω and its electric field intensity $\mathscr{E}$.

Assuming the amplitude of a high frequency electromagnetic field to be small, we find the solution of equation (14) in a one-mode approximation using the perturbation theory

$$\Psi(z,t)=\sum_{s=-1}^{+1}\Psi_s(z)\,\mathrm{e}^{-\mathrm{i}(\omega_0+s\omega)t},\qquad (\omega_0=E/\hbar),\tag{16}$$

where $\Psi_{s=0}(z)\equiv\Psi_{(\mathrm{o})}(z)$.

Preserving the first order magnitudes in equation (14), we obtain inhomogeneous equations for the corrections $\Psi_{\pm1}(z)$ to the wave functions

$$\left[H_{(\mathrm{o})}(z)-\hbar(\omega_0\pm\omega)\right]\Psi_{\pm1}(z)-e\mathscr{E}\{z\,[\theta(z)-\theta(z-b)]+b\theta(z-b)\}\Psi_0(z)=0.\tag{17}$$

Their solutions are the superpositions of functions

$$\Psi_{\pm1}(z)=\Psi_{\pm}(z)+\Phi_{\pm}(z).\tag{18}$$

The functions $\Psi_{\pm}(z)$, being the solutions of homogeneous equations, are written as

$$\begin{aligned}\Psi_{\pm}(z) &= \Psi_{\pm}^{(0)}(z)\theta(-z)+\sum_{p=1}^{N_\mathrm{W}+N_\mathrm{B}}\Psi_{\pm}^{(p)}(z)\left[\theta(z-z_{p-1})-\theta(z-z_p)\right]+\Psi_{\pm}^{(N_\mathrm{W}+N_\mathrm{B}+1)}(z)\theta(z-b)\\ &= B_{\pm}^{(0)}\mathrm{e}^{-\mathrm{i}k_{\pm}z}\theta(-z)+A_{\pm}^{(N_\mathrm{W}+N_\mathrm{B}+1)}\mathrm{e}^{\mathrm{i}K_{\pm}z}\theta(z-b)\\ &+ \sum_{p=1}^{N_\mathrm{W}+N_\mathrm{B}}\left[A_{\pm}^{(p)}\mathrm{Ai}(\xi_{\pm}^{(p)})+B_{\pm}^{(p)}\mathrm{Bi}(\xi_{\pm}^{(p)})\right]\left[\theta(z-z_{p-1})-\theta(z-z_p)\right],\end{aligned}\tag{19}$$

where

$$k_{\pm}=\hbar^{-1}\sqrt{2m_0(E\pm\Omega)},\qquad K_{\pm}=\hbar^{-1}\sqrt{2m_0[(E\pm\Omega)+V]},\qquad \Omega=\hbar\omega,$$

$$\xi_{\pm}^{(p)}(z)=\begin{cases}+\left(\dfrac{2m_1Vb^2}{\hbar^2}\right)^{\frac{1}{3}}\left[\dfrac{U-(E\pm\Omega)}{V}-\dfrac{z}{b}\right], & p=1,3,5,\dots,\\[2ex] -\left(\dfrac{2m_0Vb^2}{\hbar^2}\right)^{\frac{1}{3}}\left(\dfrac{E\pm\Omega}{V}-\dfrac{z}{b}\right), & p=2,4,6,\dots.\end{cases}\tag{20}$$

The partial solutions of inhomogeneous equations (17) have the exact analytical form

$$\begin{aligned}\Phi_{\pm}(z) &= \pi\frac{\mathscr{E}}{F}\sum_{p=1}^{N_\mathrm{W}+N_\mathrm{B}}\left\{\mathrm{Bi}(\xi_{\pm}^{(p)})\int_1^{\xi^{(p)}}\left[\eta-\kappa^{\frac{2}{3}}(z)\,\frac{U(z)-E}{V}\right]\mathrm{Ai}\left(\eta\mp\kappa^{\frac{2}{3}}(z)\,\frac{\Omega}{V}\right)\Psi_{(\mathrm{o})}^{(p)}(\eta)\,\mathrm{d}\eta\right.\\ &- \left.\mathrm{Ai}(\xi_{\pm}^{(p)})\int_1^{\xi^{(p)}}\left[\eta-\kappa^{\frac{2}{3}}(z)\,\frac{U(z)-E}{V}\right]\mathrm{Bi}\left(\eta\mp\kappa^{\frac{2}{3}}(z)\,\frac{\Omega}{V}\right)\Psi_{(\mathrm{o})}^{(p)}(\eta)\,\mathrm{d}\eta\right\}\end{aligned}\tag{21}$$

$$\times\quad\left[\theta(z-z_{p-1})-\theta(z-z_p)\right]\mp\frac{e\mathscr{E}b}{\Omega}\Psi_{(\mathrm{o})}^{(N_\mathrm{W}+N_\mathrm{B}+1)}(b)\,\theta(z-b),\tag{22}$$

where

$$\kappa(z)=\hbar^{-1}\sqrt{2m_{(\mathrm{o})}(z)b^2V}.\tag{23}$$

The conditions of the wave function $\Psi(z,t)$ and its density of current continuity at all RTS interfaces bring us to the fitting conditions similar to the equations (10) for the functions $\Psi_{\pm1}(z)$. Also, these equations define the unknown coefficients $B_{\pm}^{(p)}$, $A_{\pm}^{(p)}$ $[p=0\div(\mathrm{N_W}+\mathrm{N_B}+1)]$, and, consequently, the complete wave function $\Psi(z,t)$.

Further, considering the energy of electron-electromagnetic field interaction to be the sum of energies of electron waves, coming out of the both sides of RTS, we calculate, in quasi-classic approximation, the real part of dynamic conductivity through the densities of currents of electron waves coming out of the both sides of a nanosystem

$$\sigma(\Omega,E)=\frac{\Omega}{2be\mathscr{E}^2}\Big\{\big[j(E+\Omega,z=b)-j(E-\Omega,z=b)\big]-\big[j(E+\Omega,z=0)-j(E-\Omega,z=0)\big]\Big\}. \tag{24}$$

According to the quantum mechanics, the densities of currents are determined by the wave function

$$j(E,z)=\frac{\mathrm{i}e\hbar n_0}{2m_{(0)}(z)}\left[\Psi(E,z)\frac{\partial}{\partial z}\Psi^*(E,z)-\Psi^*(E,z)\frac{\partial}{\partial z}\Psi(E,z)\right]. \tag{25}$$

The real part of dynamic conductivity can be expressed as a sum of two terms

$$\sigma^-(\Omega,E)=\frac{\hbar\Omega n_0}{2b\,m_0\mathscr{E}^2}\left(k_+\left|B_+^{(0)}\right|^2-k_-\left|B_-^{(0)}\right|^2\right),$$
$$\sigma^+(\Omega,E)=\frac{\hbar\Omega n_0}{2b\,m_0\mathscr{E}^2}\left(K_+\left|A_+^{(N_\mathrm{W}+N_\mathrm{B}+1)}\right|^2-K_-\left|A_-^{(N_\mathrm{W}+N_\mathrm{B}+1)}\right|^2\right). \tag{26}$$

The physical sense of these partial terms [$\sigma^{\pm}(\Omega,E)$] is evident. They are caused by the electronic currents interacting with high frequency electromagnetic field in RTS and flowing out of it in forward (σ^+) and backward (σ^-) direction with respect to the incident one.

3. Discussion of the results

Using the developed theory we display such a model of plane nano-RTS, which describes the quantum transitions and transport properties of electrons best of all. It makes possible to optimize the operation of QCL by the geometric design of separate cascade active band. The numeric calculations were performed for four nanosystems: two closed models(four-barrier active band and complete cascade)and two open models(four-barrier active band and complete cascade).

In order to compare with the experimental data [3] we used the following physical parameters: $U=516$ meV, $F=68$ kV/cm, $n_0=2\cdot10^{17}$ cm^{-3} and geometrical ones, shown in figure 1. We should note that as far as almost equal sizes of all layers in the experimentally investigated cascade in the cited paper contain a small number of unitary cells (2–4) of its composition elements, the approximation of effective masses in different layers of a nanosystem would be a rough one. At the same time, the whole active band, the whole injector or the whole cascade contains dozens of unitary cells in composition elements. Thus, one can expect that the effective mass of an electron ($m=0.08\,m_e$)averaged over all three composition elements (GaAs, AlAs, InAs) is more adequate in the present physical situation.

In order to study the effect of a geometric design of a separate cascade on the operation of QCL we calculated the energy spectrum (E_n) and oscillator forces of quantum transitions ($f_{nn'}$) within the closed model, while resonance energies (E_n), lifetimes (τ_n), active conductivity ($\sigma_{nn'}$) and its partial terms ($\sigma^{\pm}_{nn'}$) — within the open model. The results are presented in figure 2, depending on the position (b_1) of inner two-barrier element between two outer barriers of an active band at the fixed sizes of all other elements of a cascade, the same as in paper [3].

The calculations prove that the dependences of electron spectra on b_1 in closed and open systems differ not more than by 0.1%. Besides, from figures 2 (a), (e) it is clear that the first three resonance energies, as functions of b_1, calculated within the model of an open four-barrier active band [figure 2 (a)] coincide with the respective resonance energies (E_1, E_2, E_3) of those three states, calculated within the model of an open complete cascade [figure 2 (e)] where the electron with maximal probability is located in the space of an active band. In figure 2 (e) one can also see the resonance energies $E_{i1}\div E_{i4}$ (thin curves) of quasi-stationary states, where the electron with a bigger probability is located in the injector part of a cascade.

Using the closed model, we calculated the oscillator forces of quantum transitions (f_{32} and f_{31}) as functions of b_1. The results are presented for the four-barrier active band [figure 2 (d)] and for the complete cascade [figure 2 (h)]. The condition of optimal QCL operation is fulfilled when the oscillator force of quantum transition f_{32} approaches its maximal magnitude. This transition occurs between the states

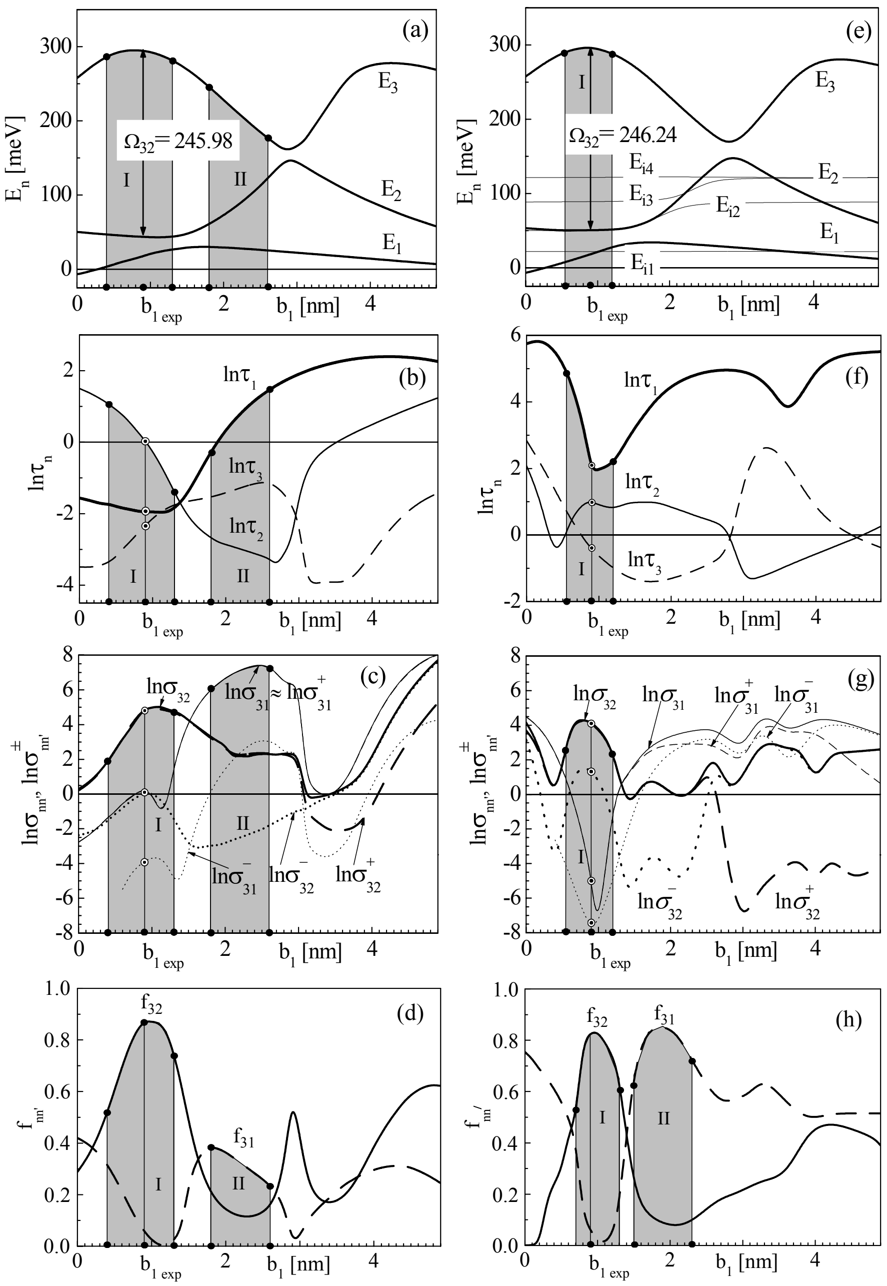

Figure 2. Electron energy spectrum (a, e), lifetimes (b, f), oscillator forces (d, h) and active conductivities (c, g) as functions of an input well width (b_1) of QCL active region in different models.

ensuring the needed energy of electromagnetic field radiation (in our case $\Omega_{32} = E_3 - E_2$). Herein, the oscillator force of quantum transition f_{31} should be an order smaller. Figure 2 (d) proves that for the four-barrier active band model, one can see two regions (I and II) of b_1 varying [toned at the figure 2 (d)] where the abovementioned condition fulfills. Herein, the I region is better than the II region because $f_{32}^{I} > f_{32}^{II}$. It is clear that the experimental point $b_{1\text{exp}}$ nearly corresponds to the maximal magnitude of f_{32} as a function of b_1. In a closed model of a complete cascade [figure 2 (h)] there is one region of b_1 varying (I) where $f_{32} > f_{31}$ and one region (II) where $f_{31} > f_{32}$. Herein, the experimental point $b_{1\text{exp}}$ also nearly coincides with b_1 corresponding to the maximal magnitude of f_{32}. The width and location of an optimal region for b_1 in this model are almost the same as in the model of a four-barrier active band.

Also, we should note that in the model of a complete cascade it seems that the QCL can operate due to the quantum transition $3 \to 1$ in the II region where $f_{31} > f_{32}$. However, as it is proven further on within the more adequate open model, this is impossible.

The resonance energies (E_n, E_{in}), lifetimes (τ_n), active conductivities (σ_{32}, σ_{31}) and their partial terms ($\sigma_{32}^{\pm}$, $\sigma_{31}^{\pm}$) are calculated as functions of b_1 for the two open models: active band [figures 2 (a), (b), (c)] and complete cascade [figures 2 (e), (f), (g)]. Before analysing the figures we should note that in the model of an active band the dynamic conductivities and their terms were calculated through the averaging over those energy regions where the levels of an injector band ($E_{i4} - E_{i1}$) are uniformly located. The calculations of these conductivities for the model of a separate complete cascade were performed taking into account that the electrons leave the previous cascade with the energy E_1, shifted at the magnitude $E_3 - E_1 - eFb$, with respect to the resonance energy E_3 of the cascade studied.

Contrary to the closed model, the open one allows for a detailed and adequate analysis of the conditions optimizing the QCL operation due to the geometric design of an active band. Within the open models, one can evaluate the magnitude of dynamic conductivity in the needed quantum transition (for example, $3 \to 2$). Besides, this conductivity would be much bigger than the conductivity of the close over the energy transition (for example, $3 \to 1$) under the condition that the partial term of conductivity (σ_{32}^{+}) in forward direction would be much bigger than the partial term (σ_{31}^{-}) in backward current. The calculated lifetimes (τ_n) of the operating electron quasi-stationary states make it possible to guide the natural physical condition: these lifetimes should not exceed the relaxation times of dissipative processes due to the scattering of electrons at the impurities, phonons, imperfections of media interfaces and other factors, which, according to the evaluations [4], are not bigger than twenty picoseconds.

The results of numeric calculations of conductivities and lifetimes of electrons in the quasi-stationary states ($n = 1,\ 2,\ 3$) obtained within the model of active band and complete cascade as functions of b_1 are presented in figures 2 (c), (b) and figures 2 (g), (f), respectively. Analysis of τ_n, $\sigma_{nn'}$, $\sigma_{nn'}^{\pm}$ dependences on b_1 [figures 2 (b), (c)] proves that there are two regions of b_1 for the model of a four-barrier active band, where: I — the optimal is the quantum transition $3 \to 2$ (experimentally observed), II — the optimal is the quantum transition $3 \to 1$. The latter transition is possible [figure 2 (c)] the same as in the model of a closed cascade. In this narrow region (II) for b_1, the lifetime in the first quasi-stationary state is rather small ($\tau_1 \leqslant 1 \div 3\,\text{ps} < 10\,\text{ps}$).

The model of an open complete cascade [figures 2 (f), (g)] is the best one for the description of the properties of an electron current through the RTS of QCL with the electromagnetic radiation accompanying quantum transitions. Figure 2 (g) proves that in this model, the same as in the model of an open active band, there are also two regions for b_1 varying (I and II) where the conditions of optimal QCL operation fulfill well (the transitions $3 \to 2$ and $3 \to 1$, respectively). The location and sizes of these regions are nearly the same as in the model of an open active band and in the model of a closed complete cascade.

However, the analysis of lifetimes τ_1, τ_2, τ_3 [figure 2 (f)] shows that in fact, the region II is not optimal because at such a geometric design the lifetime $\tau_1 \geqslant 10$ ps approaches the time of dissipative processes, breaking the coherent regime of QCL. Thus, the model of an open cascade proves that in the experimental QCL [3] it is only one narrow region (I) (0.55 nm $\leqslant b_1 \leqslant$ 1.2 nm) of the position of the inner two-barrier structure between the outer barriers of an active band, where the laser operates in an optimal regime. Only this configuration ensures that the active conductivity σ_{32} in direct current is much bigger than the other conductivities. Herein, not only the lifetimes of both operating quasi-stationary states are small ($\tau_3, \tau_2 \leqslant 2$ ps) but the lifetime of the first quasi-stationary state ($\tau_1 \leqslant 10$ ps) through which the electrons flow into the next cascade due to the interaction with phonons [3, 4], is minimal.

The geometric and physical parameters for the numeric calculations within four theoretical models were taken the same as in paper [3] in order to compare the theoretical and experimental data. These parameters are presented in figure 1 and figure 2. The numeric calculations show that in all four models the energies (E_1, E_2, E_3) of operating quasi-stationary states differ between each other not more than by 0.1%. Thus, in all models the theoretical magnitude of the energy of laser radiation $\Omega_{32} = E_3 - E_2 =$ 246 meV differs from the experimental one $\Omega_{32}^{\text{exp}} = 238.8$ meV by 3% and the difference of the energies $E_3 - E_2 = 34$ meV nearly coincides with the phonon energy in [3].

Finally, we should note that the experimental geometric design of QCL cascade [3] with the input well width $b_1 = 0.9$ nm of a four-barrier active band correlates well with the magnitude b_1 in all theoretical models because it corresponds to the close to maximal oscillator forces in closed models or dynamic conductivities in the open models. However, only the model of an open cascade is the most appropriate because it does not contain those geometric configurations of an active band, inherent to the other models, which do not ensure the optimal regime of QCL operation.

4. Conclusions

1. We developed the theory of dynamic conductivity of electrons in open multibarrier RTS driven by the constant electric field taking into account the interaction between electrons and high frequency electromagnetic field.

2. Comparing with the experimentally produced QCL having a four barrier active band of separate cascade [3] we reveal that only the model of a complete open cascade confidently ensures the optimal geometric design of the active band.

3. The developed theory of dynamic conductivity of electrons through the multibarrier RTS, after modification, can be further used to optimize the operation of QCL, QCD and other nanodevices by means of the choice of their geometric design.

References

1. Faist J. Capasso F., Sivco D.L., Sirtori C., Hutchinson A.L., Cho A.Y., Science, 1994, **264**, 553; doi:10.1126/science.264.5158.553.
2. Faist J., Capasso F., Sirtori C., Appl. Phys. Lett., 1995, **66**, 538; doi:10.1063/1.114005.
3. Sirtori C., Faist J., Capasso F., Cho A.Y., Pure Appl. Opt., 1998, **7**, 373; doi:10.1088/0963-9659/7/2/027.
4. Gmachl C., Faist J., Capasso F., Sivco D.L., Cho A.Y., Rep. Prog. Phys., 2001, **64**, 1533; doi:10.1088/0034-4885/64/11/204.
5. Giorgetta F.R., Baumann E., Hofstetter D., Manz C., Yang Q., Kohler K., Graf M., Appl. Phys. Lett., 2007, **91**, 111115; doi:10.1063/1.2784289.
6. Hofstetter D., Giorgetta F.R., Baumann E., Yang Q., Manz C., Kohler K., Appl. Phys. Lett., 2008, **94**, 221106; doi:10.1063/1.3036897.
7. Wang Q.J., Pflugl C., Diehl L., Capasso F., Edamura T., Furuta S., Yamanishi M., Kan H., Appl. Phys. Lett., 2009, **94**, 151101; doi:10.1063/1.3093476.
8. Pashkovskii A.B., JETP Lett., 2005, **82**, 210; doi:10.1134/1.2121816.
9. Pashkovskii A.B., JETP Lett., 2009, **89**, 30; doi:10.1134/S002136400901007X.
10. Elesin V.F., Kateev I.Ju., Remnev M.A., Semiconductors, 2009, **43**, 257; doi:10.1134/S1063782609020250.
11. Tkach N.V., Seti Yu.A., Low Temp. Phys., 2009, **35**, 556; doi:10.1063/1.3170931.
12. Tkach N.V., Seti Ju.A., Semiconductors, 2011, **45**, 376; doi:10.1134/S1063782611030195.

Оптимізація роботи квантового каскадного лазера геометричним дизайном каскаду у відкритих і закритих моделях

М.В. Ткач, Ю.О. Сеті, І.В. Бойко, О.М. Войцехівська

Чернівецький національний університет ім. Ю. Федьковича,
вул. Коцюбинського, 2, 58012 Чернівці, Україна

У наближенні ефективних мас і прямокутних потенціалів розвинута теорія електронної динамічної провідності плоскої багатошарової резонансно-тунельної структури у постійному електричному полі в моделі відкритої наносистеми та сил осциляторів квантових переходів у моделі закритої системи. На прикладі експериментально реалізованого квантового каскадного лазера з чотирибар’єрною активною зоною окремого каскаду показано, що саме теорія динамічної провідності у моделі відкритого каскаду найбільш адекватно описує процес випромінювання високочастотного електромагнітного поля при проходженні електронів крізь резонансно-тунельну структуру у постійному електричному полі.

Ключові слова: *резонансно-тунельна наноструктура, провідність, квантовий каскадний лазер*